

Nucleon-nucleon correlations in the extreme oxygen isotopes

S. M. Wang (王思敏),^{1,2} W. Nazarewicz,³ R. J. Charity,⁴ and L. G. Sobotka⁴

¹*Institute of Modern Physics, Fudan University, Shanghai 200433, China*

²*FRIB Laboratory, Michigan State University, East Lansing, Michigan 48824, USA*

³*Department of Physics and Astronomy and FRIB Laboratory,
Michigan State University, East Lansing, Michigan 48824, USA*

⁴*Departments of Chemistry and Physics, Washington University, St. Louis, MO 63130, USA*

(Dated: August 19, 2021)

There has been an upsurge of interest in two-nucleon decays thanks to the studies of nucleon-nucleon correlations. In our previous work, based on a novel time-dependent three-body approach, we demonstrated that the energy and angular correlations of the emitted nucleons can shed light on the structure of nucleonic pairs formed inside the nucleus. In this work, we apply the new framework to study the decay dynamics and properties of some extreme proton-rich and neutron-rich oxygen isotopes, including two-proton ($2p$) decays of $^{11,12}\text{O}$ and two-neutron ($2n$) decay of ^{26}O . Here we show that the low- ℓ components of $^{11,12}\text{O}$ wave functions, which are affected by continuum and configuration-interaction effects, strongly impact decay dynamics and asymptotic correlations. In the calculated wave functions of $^{11,12}\text{O}$, diproton and cigarlike structures merge together during the tunneling process and the resulting energy- and angular correlations are very consistent with the experimental data. The asymptotic correlations of the $2n$ decay of ^{26}O dramatically change as the two-neutron decay energy approaches the zero-energy threshold. The small reported value of Q_{2n} suggests that the $2n$ decay of this nucleus can be understood in terms of the universal phase-space limit.

Introduction.—Pairing is a ubiquitous feature of fermionic many-body systems that manifests itself in the phenomena of superfluidity and superconductivity [1–3]. Many low-energy properties of the atomic nucleus are profoundly affected by pairing between its proton and neutron constituents [4–6]. The pairing condensate present in nuclear ground states is responsible for the odd-even staggering of nuclear binding energies, which creates energetic conditions for the two-nucleon radioactivity observed in a handful of unbound rare isotopes [7–9]. However, the precise impact of pairing on the detected nucleonic pairs is largely unknown. Numerous studies have been devoted to the question of nucleon-nucleon correlations. For instance, the study of short-range correlations reveals the fundamental structure of nucleonic pairs at very high relative momenta [10]. However, Cooper pairing that has profound impact on ground-state (g.s.) properties of atomic nuclei, is a low-momentum phenomenon. The presence of pairing condensate in weakly-bound nuclei close to the particle dripline leaves a strong imprint on these systems [11] as it impacts their binding, decay modes, and other properties. Since these systems are strongly affected by the presence of low-lying scattering channels, the pairing scattering into the unbound (continuum) space is expected to play a significant role [12].

In our previous work [13], we described the $2p$ decay of ^6Be and compared it with an artificial $2n$ decay of ^6He using a recently developed time-dependent approach. By comparing the dynamics of $2p$ emission with $2n$ decay, we showed that the decay dynamics and long-range correlations are strongly impacted by both initial-state and final-state interactions [14–16]. In this Letter, we focus on heavier dripline systems, which allows us to gain more

insight into the connection between inner structure and decay properties including asymptotic correlations.

The recently discovered exotic oxygen isotope ^{11}O , with 8 protons and only 3 neutrons, has attracted significant attention due to its extreme proton-to-neutron ratio and interesting $2p$ decay characteristics [17]. Its even-even neighbor, ^{12}O , is also a $2p$ emitter [18, 19]. Its measured energy and angular $2p$ correlations [20] are rather different from those observed in ^6Be [21]. Another extreme oxygen isotope is the weakly neutron-unbound ^{26}O , with 18 neutrons, which is arguably the best current candidate for the phenomenon of $2n$ radioactivity [22–29]. The measured $2n$ correlations in ^{26}O have large uncertainties, as well as its $2n$ decay energy Q_{2n} . However, the mere existence of this threshold resonance may have some unique consequences.

In this Letter, we utilize our time-dependent approach to study the decay dynamics and resulting asymptotic correlations of $^{11,12,26}\text{O}$. By combining these results with our previous spectroscopic and structural studies [30, 31], we aim at providing a comprehensive description of the extreme oxygen isotopes by revealing their open-quantum-system nature.

Method.—In our three-body approach, the parent nucleus is described as a core (c) plus two valence nucleons (n_1, n_2). The i -th cluster ($i = c, n_1, n_2$) has the position vector \mathbf{r}_i and linear momentum \mathbf{k}_i . The three-body Hamiltonian can be written as:

$$\hat{H} = \sum_i \frac{\hat{\mathbf{p}}_i^2}{2m_i} + \sum_{i>j} \hat{V}_{ij}(\mathbf{r}_{ij}) + \hat{H}_c - \hat{T}_{\text{c.m.}} \quad (1)$$

The second sum represents the pairwise interactions between the constituents, and $\hat{T}_{\text{c.m.}}$ stands for the center-of-mass (c.m.) term. \hat{H}_c is the core Hamiltonian given

by the excitation energies of the core.

To describe three-body asymptotics and to eliminate the spurious c.m. motion, one can define the Jacobi coordinates (\mathbf{x}, \mathbf{y}) and relative momenta $(\mathbf{k}_x, \mathbf{k}_y)$ [13]. Noticing that there are two types of Jacobi coordinates (Y and T types), we use θ_k and θ'_k to denote the opening angles of $(\mathbf{k}_x, \mathbf{k}_y)$ in Y - and T -Jacobi coordinates, respectively [13]. The kinetic energy of the relative motion of the emitted nucleons is $E_{pp/nn}$, and $E_{\text{core}-p/n}$ is the kinetic energy of the core-nucleon sub-system.

The total wave function can be written as $\Psi^{J\pi} = \sum_{J_v \pi_v j_c \pi_c} [\Phi^{J_v \pi_v} \otimes \phi^{j_c \pi_c}]^{J\pi}$, where $\Phi^{J_v \pi_v}$ denotes the wave function of valence nucleons and $\phi^{j_c \pi_c}$ is the core wave function. For the core states, we assume a simple rotational picture; this allows the pair of valence nucleons to couple to the excited states of the core in a non-adiabatic way [32]. The valence wave function $\Phi^{J_v \pi_v}$ is expressed in Jacobi coordinates and expanded with hyperspherical harmonics. A supersymmetric transformation method [33] is adopted to deal with the antisymmetrization between core and valence nucleons. For simplicity, we only project out those spherical Pauli-forbidden states that correspond to the orbitals occupied by the core nucleons.

The Gamow coupled-channel (GCC) method [31, 34] is utilized to calculate the initial wave function $\Psi^{J\pi}(t=0)$, in which the hyperradial part of $\Phi^{J_v \pi_v}$ employs the Berggren basis [30, 35, 36]. As a result, configuration space is extended to the complex-momentum \hat{k} -plane. In this way, the predicted resonance has complex energy \tilde{E} . Its real part represents the mean energy of the resonance while the imaginary part corresponds to the decay width $(-\Gamma/2)$. The use of Jacobi coordinates and Berggren basis allows treatment of the inner and asymptotic regions of the Schrödinger equation on the same footing, and prevents the reflection of the wave function at the boundary.

The complex-momentum state $\Psi_{\text{GCC}}^{J\pi}(t=0)$ obtained with the GCC method is subject to purely outgoing (decaying) boundary conditions. In order to study the dynamics and asymptotic correlations of two-nucleon decay, this state can be decomposed into real-momentum scattering states using the Fourier-Bessel series expansion. The resulting $\Psi_{\text{TD}}^{J\pi}(t=0)$ is a wave packet and can be propagated within a time-dependent (TD) framework. To control the numerical precision, the time evolution operator is expanded with Chebyshev polynomials [37–39]. Since we limit the time evolution to real momentum space, the wave function can be extended to very large distances. This also helps to restore the Hermitian property of the Hamiltonian matrix and the conservation of total density. Meanwhile, the configuration mixing is involved using the same hyperspherical framework in both GCC method and TD approach. Consequently, studying the evolution of the coupled configurations allows us to analyze how the wave function structure evolves during the decay process.

Hamiltonian and model parameters.—Following our

previous work on oxygen isotopes [30, 31], in which energy spectra and decay widths of $^{11,12,26}\text{O}$ states were studied, in this work, we focus on the decay dynamics and nucleon-nucleon correlations. As $^{11,12}\text{O}$ and ^{26}O are located in very different regions of the nuclear chart, different parameters are used to describe them. For $^{11,12}\text{O}$, the core ($^{9,10}\text{C}$) is taken as a rotor, which reasonably reproduces the intruder state containing the large $s_{1/2}$ component and includes the g.s. band of the core [32] (with $j_c^\pi \leq 11/2^-$ for ^9C , and $j_c^\pi \leq 4^+$ for ^{10}C). The effective core-nucleon interaction has been taken in the form of a Woods-Saxon (WS) potential (with spin-orbit term) and a one-body Coulomb interaction with the same parameters and charge distribution as Ref. [31]. For ^{26}O , we assume that the ^{24}O core is spherical, and the WS parameters are taken from Ref. [30].

The interaction between the valence nucleons is represented by the finite-range Minnesota force with the original parameters of Ref. [40], which was fitted to the phase shifts from scattering data in a large energy range and has been widely applied to study structural properties of atomic nuclei, such as binding energies and spectra. For the valence protons, this interaction is augmented by the two-body Coulomb force.

The three-body configurations in the Jacobi coordinates are denoted by (K, ℓ_x, ℓ_y, S) , where K is the hyperspherical quantum number, ℓ is the orbital angular momentum of the corresponding Jacobi axis, and S is the total intrinsic-spin of the emitted proton (neutron) pair. Similar to Ref. [31], the calculations were carried out in a model space with $\max(\ell_x, \ell_y) \leq 7$ and for a maximal hyperspherical quantum number $K_{\text{max}} = 20$. As shown in Ref. [13], the low- ℓ continuum is crucial during the decay process. Therefore, in the hyperradial part, we used the Berggren basis for the $K < 10$ channels and the harmonic oscillator basis with the oscillator length of 1.75 fm and $N_{\text{max}} = 40$ for the higher-angular-momentum channels. For the GCC calculation of the initial state, the complex-momentum contour defining the scattering part of the Berggren basis is given by the path: $\hat{k} = 0 \rightarrow 0.3 - 0.15i \rightarrow 0.5 - 0.12i \rightarrow 1 \rightarrow 2 \rightarrow 4$ (all in fm^{-1}). For TD evolution, the inner part (< 15 fm) of the initial state is expanded and propagated with a real-momentum contour, which is $k = 0 \rightarrow 0.25 \rightarrow 0.5 \rightarrow 1 \rightarrow 2 \rightarrow 4$ (all in fm^{-1}). Each segment is discretized with 100 scattering states, which is sufficient to describe the outgoing wave function precisely. In practice, we only consider the interactions inside the sphere of radius 500 fm. Since the wave function is defined in the momentum space, and evolves from the highly localized initial wave packet, this cutoff has no practical effect on the investigated physical observables.

2p decay of proton-rich oxygen isotopes.—The proton dripline is located relatively close to the line of β stability. As a result, 2p correlation data have been obtained in several cases [20, 41]. In particular, the recently measured energy correlation of the emitted protons from the

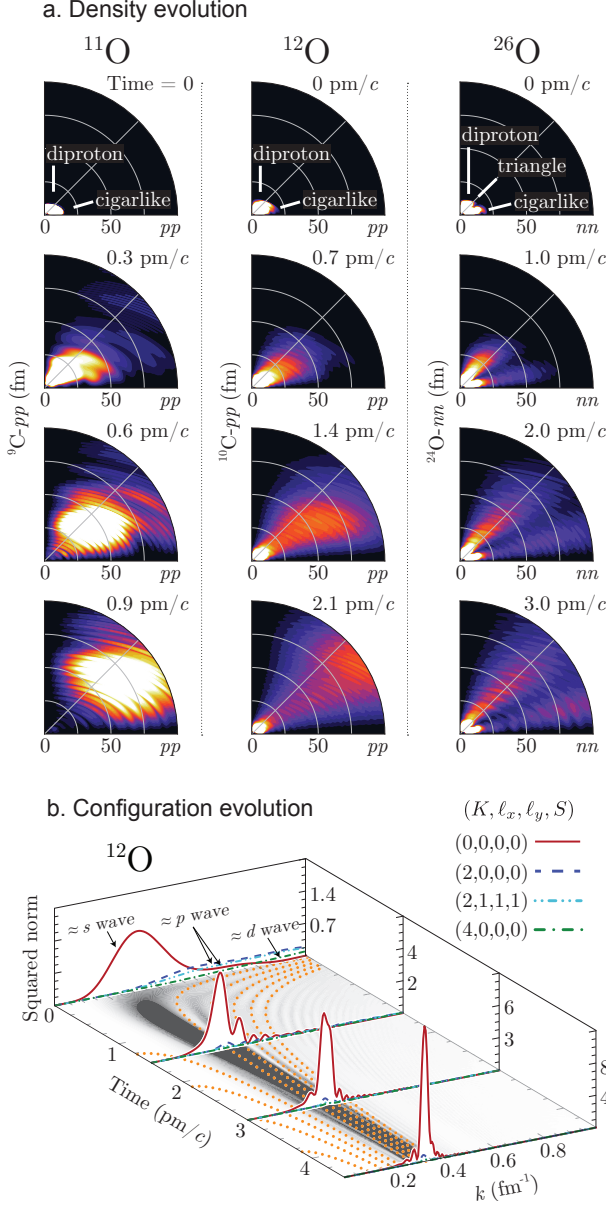


FIG. 1. (a) The density distributions of two-nucleon decays from the g.s. of oxygen isotopes for four different time slices. (b) The configuration evolution for ^{12}O . The density distributions are shown in the Jacobi- T coordinates, and multiplied by the polar Jacobi coordinate ρ to highlight the asymptotic wave function. The Jacobi- T configurations are labeled as (K, ℓ_x, ℓ_y, S) in momentum space. $k = \sqrt{k_x^2/\mu_x + k_y^2/\mu_y}$ is the total momentum and μ_x (μ_y) is the reduced mass. The projected contour map represents the sum of all the configurations, in which the interference frequencies [13] are marked by dotted lines.

g.s. of ^{12}O resembles that of ^{16}Ne (a $2p$ emitter located in the sd -shell), but dramatically differs from correlations measured in p -shell nuclei such as ^6Be [20]. This indicates there might be some structural similarity of the configurations of the valence protons in ^{12}O and ^{16}Ne .

To understand the $2p$ correlation patterns in ^{12}O and

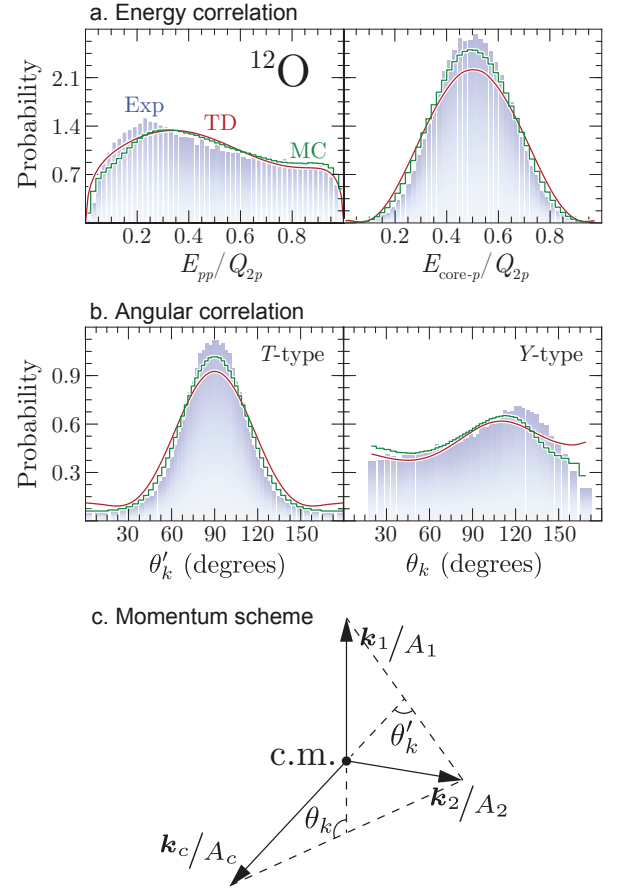


FIG. 2. Asymptotic (a) energy and (b) angular correlations of the protons emitted from the two-proton unbound ^{12}O isotope. Also shown is (c) the momentum scheme for three-body system. Theoretical distributions were obtained within the time-dependent approach (TD) at $t = 15$ pm/c. MC labels the Monte Carlo simulation of TD results which includes the experimental resolution and efficiency [20]. The calculated $2p$ correlations (TD and MC) are compared with experimental data (Exp) of Ref. [20]. A is the mass number and k_1 , k_2 , and k_c are the momenta of the nucleons n_1 and n_2 , and the core c , respectively in the c.m. coordinate frame.

neighboring ^{11}O , we applied our time-dependent approach. The initial $2p$ density in $^{11,12}\text{O}$ is indicative of a pronounced diproton and a secondary cigarlike structure [17, 31], which looks similar to that of the p -shell nuclei. However, for ^{12}O , the emitted protons originating from these configurations merge together resulting in a broad distribution seen in Fig. 1(a), which shows dramatically different decay-dynamics compared to ^6Be [13]. This result is in agreement with the calculated flux current [31], which shows a competition between diproton and cigarlike decays constituting a democratic decay.

To gain more insight into this exotic decay dynamics, we can look into the details of those configurations. The $S = 1$ component of the g.s. wave function of ^{12}O , which has the squared amplitude of 27% and allows for a more uniform distribution for the coordinate-space correlation inside the nucleus [31], is decimated asymptotically

due to the finite orbital angular momentum components. On the other hand, the weight of Jacobi- T configuration (K, ℓ_x, ℓ_y, S) = (0,0,0,0) in ^{12}O , approximately corresponding to the s -wave component, is dramatically enhanced (34% for the initial state; see Fig. 1(b)). A similar situation also occurs in ^{11}O . This is due to the appearance of s -wave threshold resonances in the neighboring nuclei $^{10,11}\text{N}$ [31]. These poles of the scattering matrix in the complex momentum plane can be viewed as analogs of antibound (virtual) states in the mirror neutron-rich partners; their existence can be also beneficial for forming the diproton structure. Due to their small centrifugal barriers, these low- ℓ components become dominant during the decay process. Figure 1(b) shows a transition in the valence-proton wave function from a structure with moderate p - and d -wave components to one that is overwhelmingly $\ell = 0$ during the $2p$ decay of ^{12}O . Indeed, the weight of the (0,0,0,0) configuration is 76% in the final state. This s -wave enhancement is partly due to the coupling to the excited core states.

The calculated asymptotic $2p$ correlations for ^{12}O shown in Fig. 2 are in qualitative, if not quantitative, agreement with experimental data. The minor differences between the experimental data and the Monte Carlo filtered calculations where the experimental acceptance and resolution is added to the time-dependent predictions could likely be reduced by modification of the employed original Minnesota force used for the nucleon-nucleon interaction. Another interesting aspect is that, unlike ^6Be (see Fig 13(a) in [20]), there is a low-energy peak in the E_{pp} correlation of ^{12}O . As distinct diproton emission during the time evolution is not expected, a low- E_{pp} correlation does not necessarily correspond to diproton decay. It is worth noting that the $2p$ system can form a subthreshold resonance with a broad decay width around 1 MeV [42]. This continuum feature is likely to affect the energy correlation of the $2p$ emitters having small decay energies.

The lightest oxygen isotope ^{11}O has been observed as a broad structure [17] containing multiple resonances [43–46]. In our previous work, four low-lying states ($J^\pi = 3/2_1^-, 5/2_1^+, 3/2_2^-,$ and $5/2_2^+$) were predicted in the experimental energy interval [31], each having a large decay width from 1 to 2 MeV. In our TD calculations, these states have been propagated individually, i.e., possible interference effects have been neglected. The large decay widths result in a strong continuum coupling, and a more uniform density distribution during the decay process compared to ^{12}O , see Fig. 1. The resulting Y -type correlations show a strong dependence on the angular momentum, which could be useful to determine experimental spin assignments. To predict the asymptotic correlations of the valence protons emitted, we combine the correlations of the four low-lying states with the weights obtained by the resonance-shape fitting [17]. This mixed correlation, shown in Fig. 3(a), captures the observed experimental features, Fig. 3(b). This agreement supports

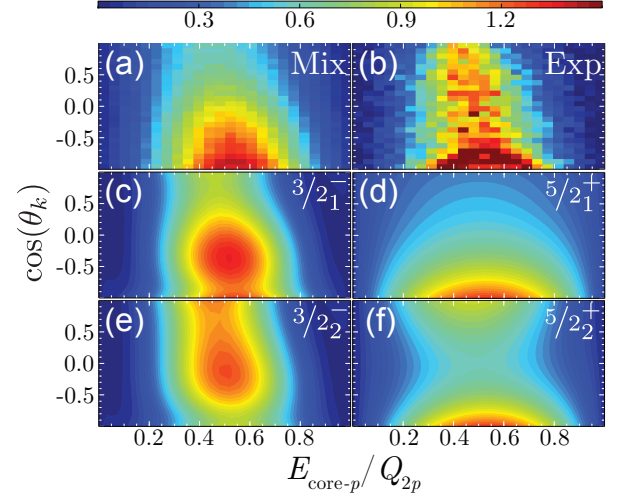


FIG. 3. (a) Theoretical and (b) experimental Jacobi- Y correlations of two protons emitted from the broad low-energy structure in ^{11}O , and (c-f) the corresponding contributions from each low-lying state predicted. The experimental resolution and efficiency have been taken into account in (a) through Monte Carlo simulations.

the argument that the observed broad structure is a mixture of $J^\pi = 3/2^-$ and $5/2^+$ states [17, 43].

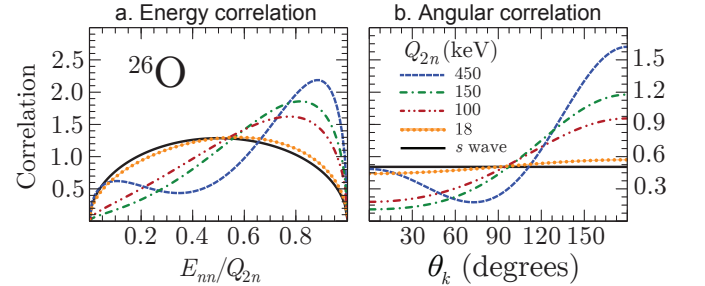


FIG. 4. Asymptotic energy (a) and angular (b) correlations of emitted neutrons from the g.s. of ^{26}O for different $2n$ decay energies Q_{2n} . Also shown are the analytical results for the asymptotic correlation in the limit of $Q_{2n} = 0$ (zero-energy s -wave). θ_k is the opening angle in the Jacobi- Y coordinate, and E_{nn} is the kinetic energy of the relative motion of the emitted neutrons.

Two-neutron decay of threshold resonance in ^{26}O .— On the neutron-rich extreme, ^{26}O is expected to decay via $2n$ emission [22–25, 28, 47]. According to our model, ^{26}O shows a very different structure, decay dynamics, and nucleon-nucleon correlation pattern as compared to the $2p$ emission from $^{11,12}\text{O}$ (see Refs. [30, 31] and Figs. 1, 2, 4).

Besides a dineutron and cigarlike structures, the initial $2n$ density of ^{26}O also contains a triangular structure. These three configurations are characteristic of the d -wave component. The very small $Q_{2n} = 18 \pm 5$ keV value [23] in ^{26}O makes this nucleus a candidate for the $2n$ radioactivity. When approaching the threshold, the pres-

ence of the centrifugal barrier is expected to give rise to changes in asymptotic correlations. As seen in Fig. 1 two branches emitted from the internal region are predicted, mainly corresponding to dineutron and large-angle configurations. The valence neutrons maintain their correlation after tunneling, which shows an enhanced large- E_{nn} correlation in Fig. 4. However, as we readjust the depth of the WS potential to bring the system closer to the experimental threshold, both energy and angular correlations of ^{26}O become almost uniformly distributed, see Fig. 4. As discussed in Ref. [28], for small values of Q_{2n} the $2n$ decay is dominated by the s -wave component and the energy distribution approaches the universal phase-space limit:

$$\frac{d\sigma}{d\varepsilon} \sim \sqrt{\varepsilon(1-\varepsilon)} \quad \text{with } \varepsilon = E_{nn}/Q_{2n}. \quad (2)$$

At the same time, the angular distribution becomes essentially isotropic. This asymptotic behavior is practically reached in our calculations for the experimental value of $Q_{2n} = 18\text{ keV}$. As the energy of the resonance increases, asymptotic energy and angular correlations quickly start deviating from the phase-space limit (2). It is seen that this deviation is already noticeable at $Q_{2n} = 100\text{ keV}$.

The appearance of s -wave dominated structures just above the reaction threshold is well known [48, 49]. When this happens, the threshold state becomes structurally aligned with the threshold and this leads to clustering effects [50]. For ^{26}O , the valence neutron pair is expected to be well decoupled from the core nucleus ^{24}O due to the very small Q_{2n} value.

Summary.—The main objective of this Letter is to investigate the connection between the inner structure of the atomic nucleus and the asymptotic correlations seen in two-nucleon decays. To this end, we studied two-proton decays of $^{11,12}\text{O}$ and two-neutron decay of ^{26}O . Through time-dependent simulations, we have demonstrated that the structure of the initial wave function, governed by the initial-state and final-state interactions can impact the decay dynamics and leave an imprint on asymptotic correlations.

Due to the configuration mixing and continuum coupling, initial wave functions of $^{11,12}\text{O}$ contain a large s -wave component. In addition, the considerable $S = 1$ part of the wave function makes the coordinate-space correlations more uniformly distributed inside the nuclei. As a result, diproton and cigarlike structures merge together during the tunneling process. These initial configurations manifest themselves in the asymptotic correlations, which show distinct patterns compared to the previously investigated case of case of ^6Be [13]. These patterns are consistent with the experimental correlation data for $^{11,12}\text{O}$.

In ^{26}O , the threshold effect dramatically changes the decay mechanism and asymptotic correlations. According to our calculations, the small reported value of $Q_{2n} =$

$18 \pm 5\text{ keV}$ suggests that the $2n$ decay of this nucleus can be understood in terms of the universal s -wave phase-space limit [28], in which the g.s. of ^{26}O attains the character of the core nucleus ^{24}O to which a pair of neutrons is weakly coupled [50].

Acknowledgements.—Discussions with Marek Płoszajczak are gratefully acknowledged. This material is based upon work supported by the U.S. Department of Energy, Office of Science, Office of Nuclear Physics under award numbers DE-SC0013365 (Michigan State University), DE-SC0018083 (NUCLEI SciDAC-4 collaboration), and DE-FG02-87ER-40316.

-
- [1] J. Bardeen, L. N. Cooper, and J. R. Schrieffer, “Theory of superconductivity,” *Phys. Rev.* **108**, 1175–1204 (1957).
 - [2] L. N. Cooper, R. L. Mills, and A. M. Sessler, “Possible superfluidity of a system of strongly interacting fermions,” *Phys. Rev.* **114**, 1377–1382 (1959).
 - [3] A. J. Leggett, “Nobel lecture: Superfluid ^3He : the early days as seen by a theorist,” *Rev. Mod. Phys.* **76**, 999–1011 (2004).
 - [4] D. M. Brink and R. A. Broglia, *Nuclear Superfluidity: pairing in finite systems (Cambridge Monographs on Particle Physics, Nuclear Physics and Cosmology)* (Cambridge University Press, New York, 2005).
 - [5] R. A. Broglia and V. Zelevinsky, *Fifty years of nuclear BCS: pairing in finite systems* (World Scientific Publishing, Singapore, 2013).
 - [6] D. J. Dean and M. Hjorth-Jensen, “Pairing in nuclear systems: from neutron stars to finite nuclei,” *Rev. Mod. Phys.* **75**, 607–656 (2003).
 - [7] V. Goldansky, “On neutron-deficient isotopes of light nuclei and the phenomena of proton and two-proton radioactivity,” *Nucl. Phys.* **19**, 482–495 (1960).
 - [8] B. Blank and M. Płoszajczak, “Two-proton radioactivity,” *Rep. Prog. Phys.* **71**, 046301 (2008).
 - [9] M. Pfützner, M. Karny, L. V. Grigorenko, and K. Riisager, “Radioactive decays at limits of nuclear stability,” *Rev. Mod. Phys.* **84**, 567–619 (2012).
 - [10] O. Hen, G. A. Miller, E. Piasetzky, and L. B. Weinstein, “Nucleon-nucleon correlations, short-lived excitations, and the quarks within,” *Rev. Mod. Phys.* **89**, 045002 (2017).
 - [11] J. Dobaczewski, N. Michel, W. Nazarewicz, M. Płoszajczak, and J. Rotureau, “Shell structure of exotic nuclei,” *Prog. Part. Nucl. Phys.* **59**, 432 (2007).
 - [12] J. Dobaczewski and W. Nazarewicz, “Hartree-Fock-Bogoliubov solution of the pairing hamiltonian in finite nuclei,” in *Fifty Years of Nuclear BCS*, edited by R. A. Broglia and V. Zelevinsky (World Scientific Publishing, Singapore, 2013) pp. 40–60.
 - [13] S. M. Wang and W. Nazarewicz, “Fermion pair dynamics in open quantum systems,” *Phys. Rev. Lett.* **126**, 142501 (2021).
 - [14] K. M. Watson, “The effect of final state interactions on reaction cross sections,” *Phys. Rev.* **88**, 1163 (1952).
 - [15] A. B. Migdal, “Theory of nuclear reactions with formation of slow particles,” *Sov. Phys. JETP* **1**, 2 (1955).
 - [16] R. Phillips, “Comparison of p-p and n-n final state interactions,” *Nucl. Phys.* **53**, 650–656 (1964).

- [17] T. B. Webb, S. M. Wang, K. W. Brown, R. J. Charity, J. M. Elson, J. Barney, G. Cerizza, Z. Chajecki, J. Estee, D. E. M. Hoff, S. A. Kuvvin, W. G. Lynch, J. Manfredi, D. McNeel, P. Morfouace, W. Nazarewicz, C. D. Pruitt, C. Santamaria, J. Smith, L. G. Sobotka, S. Sweany, C. Y. Tsang, M. B. Tsang, A. H. Wuosmaa, Y. Zhang, and K. Zhu, “First observation of unbound ^{11}O , the mirror of the halo nucleus ^{11}Li ,” *Phys. Rev. Lett.* **122**, 122501 (2019).
- [18] R. A. Kryger, A. Azhari, M. Hellström, J. H. Kelley, T. Kubo, R. Pfaff, E. Ramakrishnan, B. M. Sherrill, M. Thoennessen, S. Yokoyama, R. J. Charity, J. Dempsey, A. Kirov, N. Robertson, D. G. Sarantites, L. G. Sobotka, and J. A. Winger, “Two-proton emission from the ground state of ^{12}O ,” *Phys. Rev. Lett.* **74**, 860–863 (1995).
- [19] M. F. Jager, R. J. Charity, J. M. Elson, J. Manfredi, M. H. Mahzoon, L. G. Sobotka, M. McCleskey, R. G. Pizzone, B. T. Roeder, A. Spiridon, E. Simmons, L. Trache, and M. Kurokawa, “Two-proton decay of ^{12}O and its isobaric analog state in ^{12}N ,” *Phys. Rev. C* **86**, 011304 (2012).
- [20] T. B. Webb, R. J. Charity, J. M. Elson, D. E. M. Hoff, C. D. Pruitt, L. G. Sobotka, K. W. Brown, J. Barney, G. Cerizza, J. Estee, G. Jhang, W. G. Lynch, J. Manfredi, P. Morfouace, C. Santamaria, S. Sweany, M. B. Tsang, T. Tsang, S. M. Wang, Y. Zhang, K. Zhu, S. A. Kuvvin, D. McNeel, J. Smith, A. H. Wuosmaa, and Z. Chajecki, “Particle decays of levels in $^{11,12}\text{N}$ and ^{12}O investigated with the invariant-mass method,” *Phys. Rev. C* **100**, 024306 (2019).
- [21] I. A. Egorova, R. J. Charity, L. V. Grigorenko, Z. Chajecki, D. Coupland, J. M. Elson, T. K. Ghosh, M. E. Howard, H. Iwasaki, M. Kilburn, J. Lee, W. G. Lynch, J. Manfredi, S. T. Marley, A. Sanetullaev, R. Shane, D. V. Shetty, L. G. Sobotka, M. B. Tsang, J. Winkelbauer, A. H. Wuosmaa, M. Youngs, and M. V. Zhukov, “Democratic decay of ^6Be exposed by correlations,” *Phys. Rev. Lett.* **109**, 202502 (2012).
- [22] Z. Kohley, T. Baumann, G. Christian, P. A. DeYoung, J. E. Finck, N. Frank, B. Luther, E. Lunderberg, M. Jones, S. Mosby, J. K. Smith, A. Spyrou, and M. Thoennessen, “Three-body correlations in the ground-state decay of ^{26}O ,” *Phys. Rev. C* **91**, 034323 (2015).
- [23] Y. Kondo, T. Nakamura, R. Tanaka, R. Minakata, S. Ogoshi, N. A. Orr, N. L. Achouri, T. Aumann, H. Baba, F. Delaunay, P. Doornenbal, N. Fukuda, J. Gibelin, J. W. Hwang, N. Inabe, T. Isobe, D. Kameda, D. Kanno, S. Kim, N. Kobayashi, T. Kobayashi, T. Kubo, S. Leblond, J. Lee, F. M. Marqués, T. Motobayashi, D. Murai, T. Murakami, K. Muto, T. Nakashima, N. Nakatsuka, A. Navin, S. Nishi, H. Otsu, H. Sato, Y. Satou, Y. Shimizu, H. Suzuki, K. Takahashi, H. Takeda, S. Takeuchi, Y. Togano, A. G. Tuff, M. Vandebrouck, and K. Yoneda, “Nucleus ^{26}O : A barely unbound system beyond the drip line,” *Phys. Rev. Lett.* **116**, 102503 (2016).
- [24] L. V. Grigorenko, I. G. Mukha, and M. V. Zhukov, “Lifetime and fragment correlations for the two-neutron decay of ^{26}O ground state,” *Phys. Rev. Lett.* **111**, 042501 (2013).
- [25] K. Hagino and H. Sagawa, “Correlated two-neutron emission in the decay of the unbound nucleus ^{26}O ,” *Phys. Rev. C* **89**, 014331 (2014).
- [26] A. Adahchour and P. Descouvemont, “Three-body continuum of ^{26}O ,” *Phys. Rev. C* **96**, 054319 (2017).
- [27] K. Fossez, J. Rotureau, N. Michel, and W. Nazarewicz, “Continuum effects in neutron-drip-line oxygen isotopes,” *Phys. Rev. C* **96**, 024308 (2017).
- [28] L. V. Grigorenko, J. S. Vaagen, and M. V. Zhukov, “Exploring the manifestation and nature of a dineutron in two-neutron emission using a dynamical dineutron model,” *Phys. Rev. C* **97**, 034605 (2018).
- [29] J. G. Li, N. Michel, W. Zuo, and F. R. Xu, “Unbound spectra of neutron-rich oxygen isotopes predicted by the Gamow shell model,” *Phys. Rev. C* **103**, 034305 (2021).
- [30] S. M. Wang, N. Michel, W. Nazarewicz, and F. R. Xu, “Structure and decays of nuclear three-body systems: The Gamow coupled-channel method in Jacobi coordinates,” *Phys. Rev. C* **96**, 044307 (2017).
- [31] S. M. Wang, W. Nazarewicz, R. J. Charity, and L. G. Sobotka, “Structure and decay of the extremely proton-rich nuclei $^{11,12}\text{O}$,” *Phys. Rev. C* **99**, 054302 (2019).
- [32] B. Barmore, A. T. Kruppa, W. Nazarewicz, and T. Vertse, “Theoretical description of deformed proton emitters: Nonadiabatic coupled-channel method,” *Phys. Rev. C* **62**, 054315 (2000).
- [33] J.-M. Sparenberg and D. Baye, “Supersymmetry between phase-equivalent coupled-channel potentials,” *Phys. Rev. Lett.* **79**, 3802–3805 (1997).
- [34] S. M. Wang and W. Nazarewicz, “Puzzling two-proton decay of ^{67}Kr ,” *Phys. Rev. Lett.* **120**, 212502 (2018).
- [35] T. Berggren, “On the use of resonant states in eigenfunction expansions of scattering and reaction amplitudes,” *Nucl. Phys. A* **109**, 265–287 (1968).
- [36] N. Michel, W. Nazarewicz, M. Płoszajczak, and T. Vertse, “Shell model in the complex energy plane,” *J. Phys. G* **36**, 013101 (2009).
- [37] A. Volya, “Time-dependent approach to the continuum shell model,” *Phys. Rev. C* **79**, 044308 (2009).
- [38] Y. L. Loh, S. N. Taraskin, and S. R. Elliott, “Fast Chebyshev-polynomial method for simulating the time evolution of linear dynamical systems,” *Phys. Rev. E* **63**, 056706 (2001).
- [39] T. Ikegami and S. Iwata, “Spectral density calculation by using the Chebyshev expansion,” *J. Comput. Chem.* **23**, 310–318 (2002).
- [40] D. Thompson, M. Lemere, and Y. Tang, “Systematic investigation of scattering problems with the resonating-group method,” *Nucl. Phys. A* **286**, 53–66 (1977).
- [41] K. Miernik, W. Dominik, Z. Janas, M. Pfützner, L. Grigorenko, C. R. Bingham, H. Czyrkowski, M. Ćwiok, I. G. Darby, R. Dąbrowski, T. Ginter, R. Grzywacz, M. Karny, A. Korgul, W. Kuśmierz, S. N. Liddick, M. Rajabali, K. Rykaczewski, and A. Stolz, “Two-proton correlations in the decay of ^{45}Fe ,” *Phys. Rev. Lett.* **99**, 192501 (2007).
- [42] L. P. Kok, “Accurate determination of the ground-state level of the ^2He nucleus,” *Phys. Rev. Lett.* **45**, 427–430 (1980).
- [43] T. B. Webb, R. J. Charity, J. M. Elson, D. E. M. Hoff, C. D. Pruitt, L. G. Sobotka, K. W. Brown, J. Barney, G. Cerizza, J. Estee, W. G. Lynch, J. Manfredi, P. Morfouace, C. Santamaria, S. Sweany, M. B. Tsang, T. Tsang, Y. Zhang, K. Zhu, S. A. Kuvvin, D. McNeel, J. Smith, A. H. Wuosmaa, and Z. Chajecki, “Invariant-mass spectrum of ^{11}O ,” *Phys. Rev. C* **101**, 044317 (2020).
- [44] H. T. Fortune, “Energy and width of $^{11}\text{O(g.s.)}$,” *Phys. Rev. C* **99**, 051302 (2019).
- [45] E. Garrido and A. S. Jensen, “Few-body structures in the mirror nuclei ^{11}O and ^{11}Li ,” *Phys. Rev. C* **101**, 034003 (2020).

- (2020).
- [46] X. Mao, J. Rotureau, W. Nazarewicz, N. Michel, R. M. Id Betan, and Y. Jaganathen, “Gamow-shell-model description of Li isotopes and their mirror partners,” *Phys. Rev. C* **102**, 024309 (2020).
 - [47] K. Hagino and H. Sagawa, “Decay dynamics of the unbound ^{25}O and ^{26}O nuclei,” *Phys. Rev. C* **93**, 034330 (2016).
 - [48] E. P. Wigner, “On the behavior of cross sections near thresholds,” *Phys. Rev.* **73**, 1002–1009 (1948).
 - [49] F. C. Barker, “A model for nuclear threshold levels,” *Proc. Phys. Soc.* **84**, 681 (1964).
 - [50] J. Okołowicz, M. Płoszajczak, and W. Nazarewicz, “Convenient location of a near-threshold proton-emitting resonance in ^{11}B ,” *Phys. Rev. Lett.* **124**, 042502 (2020).